Frontiers of Information Technology & Electronic Engineering
www.jzus.zju.edu.cn; engineering.cae.cn; www.springerlink.com
ISSN 2095-9184 (print); ISSN 2095-9230 (online)
E-mail: jzus@zju.edu.cn

Multi-focus image fusion based on fractional-order derivative and intuitionistic fuzzy sets

Xue-feng ZHANG†‡, Hui YAN, Hao HE

School of Sciences, Northeastern University, Shenyang 110819, China

†E-mail: zhangxuefeng@mail.neu.edu.cn

Received Dec. 28, 2019; Revision accepted Feb. 15, 2020; Crosschecked Mar. 26, 2020

Abstract: Multi-focus image fusion is an increasingly important component in image fusion, and it plays a key role in imaging. In this paper, we put forward a novel multi-focus image fusion method which employs fractional-order derivative and intuitionistic fuzzy sets. The original image is decomposed into a base layer and a detail layer. Furthermore, a new fractional-order spatial frequency is built to reflect the clarity of the image. The fractional-order spatial frequency is used as a rule for detail layers fusion, and intuitionistic fuzzy sets are introduced to fuse base layers. Experimental results demonstrate that the proposed fusion method outperforms the state-of-the-art methods for multi-focus image fusion.

Key words: Image fusion; Fractional-order derivative; Intuitionistic fuzzy sets; Multi-focus images
https://doi.org/10.1631/FITEE.1900737 **CLC number:** TP302.4

1 Introduction

As an important branch of information fusion, image fusion is a research hotspot (Zhang L et al., 2010; Chen Y and Qin, 2015; Zhu et al., 2017). Image fusion is mainly to fuse the information of multiple images in matrix form into a single image. The information of the fused image is more comprehensive, and more suitable for human visual observation and computer post-processing. As a comprehensive technique, image fusion has been widely used in medical, military, and remote sensing fields.

Multi-focus image fusion refers to the fusion of images with different focuses to obtain an image with two clear targets (Huang and Jing, 2007). Because of the limited optical lens, it is difficult to obtain a clear panoramic image with photography. Therefore, it is necessary to fuse two multi-focus images with different blurred areas and clear areas. Generally, multi-focus image fusion can be divided into three levels, i.e., pixel, feature, and decision levels. Among them, the pixel level is the easiest and the information of the fusion image is the richest without losing the information of the original images. The pixel-level multi-focus image fusion algorithm based on the spatial domain is to analyze and process image pixels directly. This kind of algorithm can save as much as possible data of the source image, and its calculation is relatively simple.

In recent years, many multi-focus image fusion methods have been proposed. In particular, spatial frequency (SF), which refers to the quality of the image region focus, has been introduced into image fusion. Li et al. (2001) combined SF with image decomposition to fuse images effectively. Then, Li and Yang (2008) proposed multi-focus image fusion algorithms based on region segmentation and SF. The traditional segmentation algorithm was used to divide images into different regions, and then the SF of the corresponding region was used to fuse images. In Yang B and Li (2007), SF was segmented directly. The above methods segment the source images into

‡ Corresponding author
ORCID: Xue-feng ZHANG, https://orcid.org/0000-0002-2831-5747

regions which can represent the characteristics of the images, and then use SF to fuse images.

Although the results of the above fusion methods reflect the feature information of source images very well in vision, the fusion results have a strong dependence on segmentation effects in practical applications. Li et al. (2013) proposed a method based on two-scale image decomposition: an image is divided into a base layer and a detail layer, and then the guided filtering-based weighted average technique is used to fuse images effectively. Compared with the image fusion methods based on regional features, the fusion method based on image layering is more sensitive to image details, and it can overcome the disadvantage of the uncertainty of segmentation regions.

Fuzzy sets (FSs) constitute a theory which aims at dealing with fuzzy and uncertain things and quantifies them as the information that can be processed by computer (Zadeh, 1965). Atanassov (1986) expanded FS to intuitionistic fuzzy sets (IFSs). IFS takes account of the information of membership, non-membership, and hesitation degrees at the same time, so it is more flexible and practical than traditional FSs in dealing with fuzziness and uncertainty. Many image fusion problems have been solved using IFS. Specifically, Yang Y et al. (2016) proposed a method to fuse images in IFS. It is more suitable for image fusion since images have a lot of uncertainties.

Fractional calculus, which is a theory of fractional order, has been widely used to deal with many practical problems on image processing, such as image denoising, image enhancement, and image super-resolution (Bai and Feng, 2007; Pu YF et al., 2010; Chen DL et al., 2015). Compared with traditional local integral calculus, fractional calculus has the property of non-locality. This means that fractional calculus is related to not local information, but the whole range of discussion. Thus, fractional calculus has the advantage of memorability. Because of the property of non-locality, the application of fractional calculus to image processing can describe more vividly image features such as edges, textures, and smooth areas. Some researchers also applied it to image fusion and obtained effective fusion results (Azarang and Ghassemian, 2018), but no one has introduced it into the clarity measure of images to fuse images. Therefore, we apply fractional calculus to the clarity measure to perfectly describe the clarity information of images, so as to fuse images.

In this study, we combine IFS and fractional-order derivative to produce a novel method for multi-focus image fusion. To better preserve the details of the original images, two-scale representations of the original images are first obtained according to an average filter. Then, the base layers are fused through IFS, making full use of the richness of gray values of images. To reflect the clarity of images, the fractional-order spatial frequency (FSF) is built which is an integration of fractional-order derivative and SF. FSF is used to fuse detail layers capturing small-scale details.

2 Preliminaries

2.1 Fractional-order derivative

In this subsection, definitions and properties of the fractional-order derivative are introduced. There are three popular definitions of the fractional-order derivative, i.e., Riemann-Liouville (R-L), Caputo, and Grünwald-Letnikov (G-L) (Podlubny, 1999; Zhang XF and Chen, 2018). The G-L definition is introduced in this study. The definition of the G-L fractional differential of order α is

$$\begin{aligned} &D^{\alpha}_{\text{G-L}}u(x):\frac{\mathrm{d}^{\alpha}}{\mathrm{d}x^{\alpha}}u(x)|_{\text{G-L}}\\ &:=\lim_{n\to\infty}\left(\frac{\left(\frac{x}{n}\right)^{-\alpha}}{\Gamma(-\alpha)}\sum_{k=0}^{n-1}\frac{\Gamma(k-\alpha)}{\Gamma(k+1)}u\left(x-k\left(\frac{x}{n}\right)\right)\right), \end{aligned} \tag{1}$$

where $u(x)$ is the signal under consideration, α is a real number, and $\Gamma(\cdot)$ is the Gamma function.

Based on the G-L definition, the discrete derivative definition can be given. The fractional-order discretized derivative at point (i,j) along the x and y directions are as follows:

$$D^{\alpha}_{x}u_{ij}=\sum_{k=0}^{i+1}w^{\alpha}_{k}u_{i-k+1,j},\ i,j=1,2,\ldots,n,$$

$$D^{\alpha}_{y}u_{ij}=\sum_{k=0}^{j+1}w^{\alpha}_{k}u_{i,j-k+1},\ i,j=1,2,\ldots,n,$$

where

$$w^{\alpha}_{k}=(-1)^{k}\frac{\Gamma(\alpha+1)}{\Gamma(k+1)\Gamma(\alpha-k+1)}$$

and $k=0,1,\ldots,n+1$. The coefficients w^{α}_{k} can be

obtained through the recursive relation:

$$w_k^\alpha = \begin{cases} 1, & k=0, \\ \left(1-\dfrac{\alpha+1}{k}\right) w_{k-1}^\alpha, & k=1,2,\ldots,n+1. \end{cases}$$

Then the discrete α-order gradient can be written in the following matrix form:

$$D^\alpha \boldsymbol{u} = \begin{pmatrix} D_x^\alpha \boldsymbol{u} \\ D_y^\alpha \boldsymbol{u} \end{pmatrix} = \begin{pmatrix} \boldsymbol{Mu} \\ \boldsymbol{uM} \end{pmatrix} \in \mathbb{R}^{2n\times n}, \tag{2}$$

where

$$\boldsymbol{M} = \begin{pmatrix} w_1^\alpha & 0 & 0 & \cdots & 0 \\ w & w_1^\alpha & \ddots & \ddots & \vdots \\ w_3^\alpha & \ddots & \ddots & \ddots & 0 \\ \vdots & \ddots & \ddots & w_1^\alpha & 0 \\ w_n^\alpha & \cdots & w_3^\alpha & w & w_1^\alpha \end{pmatrix} \in \mathbb{R}^{n\times n} \tag{3}$$

and $w = w_0^\alpha + w_2^\alpha$.

Then, considering signal processing and the fractional-order derivative, the definition of the Fourier transform of $u(x)$ (Tao et al., 2006) is as follows:

$$\begin{aligned} \mathrm{FT}\left(D^\alpha u(x)\right) =& (\mathrm{i}\omega)^\alpha \mathrm{FT}(u(x)) \\ & - \sum_{k=0}^{n-1} (\mathrm{i}\omega)^k \frac{\mathrm{d}^{\alpha-1-k}}{\mathrm{d}x^{\alpha-1-k}} u(0), \end{aligned} \tag{4}$$

where i is the imaginary unit and ω is the digital frequency. When $u(x)$ is a causal signal, Eq. (4) can be written as

$$\mathrm{FT}(D^\alpha s(x)) = (\mathrm{i}\omega)^\alpha \mathrm{FT}(s(x)).$$

Fig. 1 shows the amplitude-frequency figure, which is the fractional Fourier transform of different orders. In Fig. 1, we can see that the fractional-order differential operator can enhance the low-frequency signal to a certain extent when the fractional order belongs to $(0,1)$, and that the amplitude of enhancement is larger than that of the first- and second-order differential operators (Pu YF and Wang, 2007). At high frequencies of the signal, the fractional-order operator also enhances the signal. Although the enhancement amplitude is not as large as that of the first and second orders, the fractional-order signal enhances the low-frequency signal at the same time. It is shown that the fractional-order differential has weak derivatives, which not only increases the high frequency of the signal, but also preserves the low frequency nonlinearly.

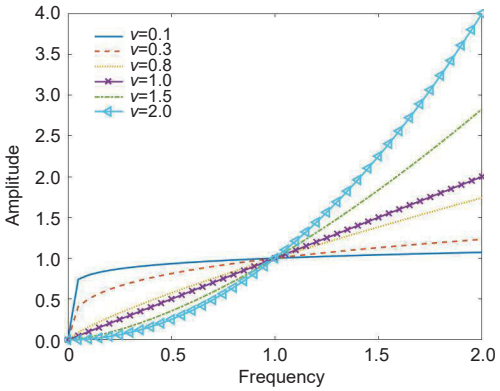

Fig. 1 Amplitude-frequency characteristic curves of fractional-order differential operators (v: fractional order)

2.2 Intuitionistic fuzzy sets

IFS has been widely used in image processing and is described in this subsection (Xu, 2007).

Consider a finite set $S = \{s_1, s_2, \ldots, s_n\}$. A fuzzy set F of S is defined as

$$F = \{(s, \mu_F(s)) | s \in S\}, \tag{5}$$

where the function $\mu_F(s) : F \to [0,1]$ denotes the membership degree of s in S. Thus, the non-membership degree of s is written as $1-\mu_F(s)$.

Atanassov (1986) put forward IFS on the basis of FS, considering the information of membership, non-membership, and the hesitation degree at the same time. IFS is defined as

$$F = \{(s, \mu_F(s), \nu_F(s)) | s \in S\}, \tag{6}$$

where $\mu_F(s), \nu_F(s) : F \to [0,1]$ denote the membership degree and non-membership degree of an element s in S respectively, and the condition $0 \le \mu_F(s) + \nu_F(s) \le 1$ holds.

Then, hesitation degree $\pi_F(s)$ is introduced in relation to the lack of knowledge. IFS is defined based on the hesitation degree, written as

$$F = \{(s, \mu_F(s), \nu_F(s), \pi_F(s)) | s \in S\}, \tag{7}$$

where $\mu_F(s) + \nu_F(s) + \pi_F(s) = 1$.

3 Fractional-order spatial frequency

In Eskicioglu and Fisher (1995), spatial frequency was used to measure the overall activity level in images. Then, Li et al. (2001) proved that the

spatial frequency can describe the clarity of images. The definition of SF is

$$\mathrm{SF}=\sqrt{\mathrm{RF}^2+\mathrm{CF}^2}, \tag{8}$$

$$\mathrm{RF}=\sqrt{\frac{1}{JK}\sum_{m=1}^{J}\sum_{n=2}^{K}(f(m,n)-f(m,n-1))^2}, \tag{9}$$

$$\mathrm{CF}=\sqrt{\frac{1}{JK}\sum_{m=2}^{J}\sum_{n=1}^{K}(f(m,n)-f(m-1,n))^2}, \tag{10}$$

where $[J,K]$ is the size of image block $\boldsymbol{f}$. From the definition of SF, $f(m,n)-f(m,n-1)$ and $f(m,n)-f(m-1,n)$ can be seen as the partial derivatives of $\boldsymbol{f}$ at point (m,n) along the x and y directions. From the definitions of fractional- and integer-order derivatives, the integer-order derivative combines only the value in the current step with those in a finite number of previous steps, and the fractional-order derivative is related to all the values in the range. Thus, the fractional-order derivative has the advantage of memorability. Furthermore, the fractional-order derivative can highlight details of image textures. It is more sensitive to different features of an image than the integer-order derivative. Based on the advantages of the fractional-order derivative, we define the FSF as follows:

$$\mathrm{FSF}=\sqrt{\mathrm{FRF}^2+\mathrm{FCF}^2}=\|D^{\alpha}\boldsymbol{f}\|_{\mathrm{F}}, \tag{11}$$

$$\mathrm{FRF}=\|\boldsymbol{M}\boldsymbol{f}\|_{\mathrm{F}}, \tag{12}$$

$$\mathrm{FCF}=\|\boldsymbol{f}\boldsymbol{M}\|_{\mathrm{F}}, \tag{13}$$

where $\boldsymbol{M}$ is the coefficient matrix of the fractional-order derivative as in Eq. (3) and $\|\cdot\|_{\mathrm{F}}$ denotes the Frobenius norm.

Figs. 2b–2f are "Lena" blocks after blurring with a Gaussian of radius 0.5, 0.51, 0.8, 1.0, and 1.5, respectively, while Fig. 2a is the original block. Table 1 shows the SF and FSF of the images in Fig. 2, where α of FSF is 1.5 or 0.5. From the results above, with the images more blurred, SF and FSF become smaller gradually. The experimental results show that SF and FSF are consistent with human visual perception of blur. The more blurred the images, the smaller the corresponding values. Thus, both can be used to reflect the clarity of images.

To compare the sensitivity of SF and FSF, we set up a special group of experiments. Setting the blur radius to 0.5 and 0.51, their corresponding SF and FSF values are given in Table 1. The change of SF is about 0.1363, and the change of FSF is larger than that of SF when $\alpha=1.5$. Combining fractional order has the advantages of memorability and detailed description of the image. We can conclude that FSF has better perception of clarity than SF.

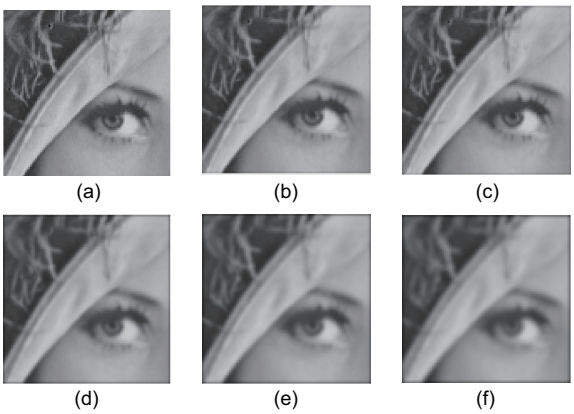

Fig. 2 Original (a) and blurred versions of block "Lena" with radius 0.5 (b), 0.51 (c), 0.8 (d), 1.0 (e), and 1.5 (f)

Table 1 Spatial frequency (SF) and fractional-order spatial frequency (FSF) of the images in Fig. 2

Radius	SF	FSF ($\alpha=1.5$)	FSF ($\alpha=0.5$)
0	18.3581	28.3781	28.7471
0.5	15.3249	24.5047	27.2160
0.51	15.1886	24.3370	27.1395
0.8	13.1816	21.8856	25.8097
1.0	12.3307	20.7671	25.2856
1.5	11.2530	19.3123	24.6474

4 Model description

The details of the fusion method are described in this section. Suppose that the two original multi-focus images $\boldsymbol{u}_1$ and $\boldsymbol{u}_2$ are pre-registered. The framework of the method proposed is shown in Fig. 3. First, average filtering decomposes $\boldsymbol{u}_1$ and $\boldsymbol{u}_2$ into base layers $\boldsymbol{B}_1, \boldsymbol{B}_2$ and detail layers $\boldsymbol{D}_1, \boldsymbol{D}_2$, respectively. Then the base layers are fused by IFS and the detail layers are fused by FSF. Finally, the target image is obtained according to the combination of the processed base and detail layers.

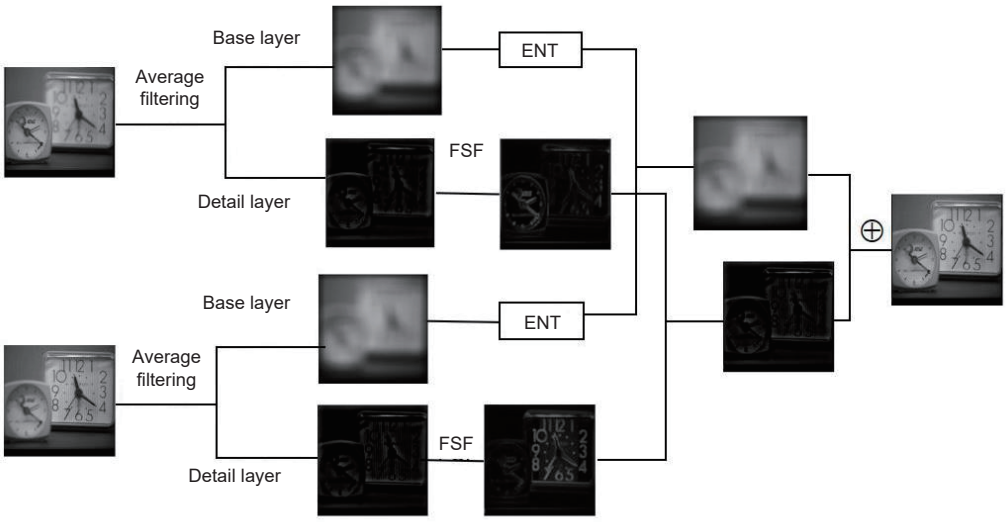

Fig. 3 Flow diagram of the proposed multi-focus image (ENT: fuzzy entropy)

4.1 Two-scale image decomposition

As shown in Fig. 3, average filtering is used to decompose the original images into two-scale representations. The base layer is obtained as follows:

$$\boldsymbol{B}_n = \boldsymbol{u}_n * \boldsymbol{Z},\ n = 1, 2, \tag{14}$$

where $\boldsymbol{u}_n$ $(n = 1, 2)$ is the original image, and $\boldsymbol{Z}$ is average filtering, whose size is 30×30. Based on the base layer, the detail layer can be obtained easily:

$$\boldsymbol{D}_n = \boldsymbol{u}_n - \boldsymbol{B}_n,\ n = 1, 2. \tag{15}$$

The purpose of two-scale decomposition is to segment each source image into a base layer and a detail layer. The base layer contains large-scale changes in the image, and the detail layer contains small-scale details. Two-scale decomposition divides each source image into two scales, and each scale contains different information. This makes the later fusion information more comprehensive and specific, and makes the fusion rules more targeted.

The base layer reflects the large-scale information about the source image. Because the two base layers of the source images are very fuzzy, the difference of sharpness is not obvious. Therefore, we use the entropy of images, which represents the richness of image information and IFS, to fuse them. This fusion method can make full use of uncertainties of source images, and fuse the basic information effectively.

4.2 Base layer fusion with IFS

On the basis of IFS, the membership $\mu(i, j)$ can fuzzily denote the belongingness of the gray value of images, defined as (Balasubramaniam and Ananthi, 2014)

$$\mu(i, j) = \frac{u(i, j) - a}{b - a}, \tag{16}$$

where $u(i, j)$ is the gray value of the image, $a = \min(u)$, and $b = \max(u)$.

Then, the membership degree of IFS based on Eq. (16) is defined as

$$\mu_{\mathrm{IFS}}(i, j) = 1 - (1 - \mu(i, j))^{\lambda},\ \lambda \geq 0. \tag{17}$$

The non-membership degree is calculated as

$$\nu_{\mathrm{IFS}}(i, j) = (1 - \mu(i, j))^{\lambda(\lambda+1)},\ \lambda \geq 0. \tag{18}$$

The hesitation degree is computed as follows:

$$\pi_{\mathrm{IFS}}(i, j) = 1 - \mu_{\mathrm{IFS}}(i, j) - \nu_{\mathrm{IFS}}(i, j). \tag{19}$$

Fuzzy entropy measures the uncertainty of a fuzzy set. The larger the fuzzy entropy is, the more abundant the information it contains. Therefore, it is necessary and effective to use the maximum value of fuzzy entropy to determine λ. In this study, the fuzzy entropy is described as

$$\mathrm{ENT}(\mathrm{IFS}, \lambda) = \frac{1}{MN} \sum_{m=1}^{M} \sum_{n=1}^{N} \frac{V}{U}, \tag{20}$$

where

$$V = 2\mu_{\mathrm{IFS}}\nu_{\mathrm{IFS}} + \pi^2_{\mathrm{IFS}},$$
$$U = \mu^2_{\mathrm{IFS}} + \nu^2_{\mathrm{IFS}} + \pi^2_{\mathrm{IFS}},$$

and $M \times N$ represents the window size 5×5.

Therefore, we fuse the base layers with fuzzy entropy, and this represents the richness of the information contained in the image. The fusion rule for the base layers is as follows:

$$B(i,j) = \begin{cases} B_1(i,j), & \mathrm{ENT}_1(i,j) \geq \mathrm{ENT}_2(i,j), \\ B_2(i,j), & \text{otherwise.} \end{cases} \tag{21}$$

4.3 Detail layer fusion with FSF

The detail layers can reflect the information about the source images in detail, including edges, textures, and other abrupt information. The frequency of these layers is high, and the difference of the gray values for multi-focus images is obvious. Thus, it is suitable for fusing images based on FSF, which can fuse frequency information easily.

First, we use Eq. (11) to calculate the FSF of position (i, j) in the 5×5 window. Then, the fusion rule for the detail layers is built according to the max-min operator, written as follows:

$$D(i,j) = \begin{cases} D_1(i,j), & \mathrm{FSF}_1(i,j) \geq \mathrm{FSF}_2(i,j), \\ D_2(i,j), & \text{otherwise.} \end{cases} \tag{22}$$

4.4 Two-scale image reconstruction

Through the above steps, we can obtain the fused base layer and detail layer. Finally, the two layers of the source image are added to obtain the complete fusion image:

$$\boldsymbol{u} = \boldsymbol{B} + \boldsymbol{D}. \tag{23}$$

4.5 Choice of variable order

Image processing of a variable fractional order is to construct an independent optimization framework of images by selecting independent evaluation indices. This is of great practical significance (Baleanu and Wu, 2019; Wu et al., 2019). We use the adaptive feedback method to fuse images. Entropy (EN) is used as the evaluation index of image fusion, and the fractional order in the range of (1,2) is the fusion parameter. By calculating the EN of the fused image with different fractional orders, the fused image corresponding to the largest EN is selected as the final result. All fusion parameters are optimized by taking the EN of the final fusion image as the objective function. This method can not only ensure the robustness of the proposed method, but also obtain the optimal fusion image.

5 Experimental results

To demonstrate the performance of the proposed method, several experiments are given and analyzed in this section.

5.1 Performance index

Entropy (EN), mutual information (MI), and average gradient (AVG) are used to evaluate the quality of the fused multi-focus images. EN is used to measure the amount of information contained in an image. The larger the EN, the greater the amount of information contained in an image and the richer the image information. EN is defined as follows:

$$\mathrm{EN} = -\sum_{i=0}^{L-1} p_i \cdot \log_2 p_i,$$

where $L = 256$ and p_i is the distribution probability of each gray level.

MI is an important index to calculate how much information the source image has transferred to the fusion image. MI shows the completeness of the fusion image. Thus, the larger the MI, the better the fusion effect. MI is defined by

$$\mathrm{MI} = \mathrm{MI}_{1\mathrm{U}} + \mathrm{MI}_{2\mathrm{U}},$$
$$\mathrm{MI}_{1\mathrm{U}} = \sum_{\boldsymbol{u},1} P_{1\mathrm{U}} f(\boldsymbol{u}, \boldsymbol{u}_1) \lg \frac{P_{1\mathrm{U}}(\boldsymbol{u}, \boldsymbol{u}_1)}{P_1(\boldsymbol{u}_1) P_{\mathrm{U}}(\boldsymbol{u})},$$
$$\mathrm{MI}_{2\mathrm{U}} = \sum_{\boldsymbol{u},2} P_{2\mathrm{U}} f(\boldsymbol{u}, \boldsymbol{u}_2) \lg \frac{P_{2\mathrm{U}}(\boldsymbol{u}, \boldsymbol{u}_2)}{P_2(\boldsymbol{u}_2) P_{\mathrm{U}}(\boldsymbol{u})},$$

where $P_1(\boldsymbol{u}_1)$ and $P_2(\boldsymbol{u}_2)$ are the edge probability densities of $\boldsymbol{u}_1$ and $\boldsymbol{u}_2$ respectively, $P_{\mathrm{U}}(\boldsymbol{u})$ is the probability density of fusion image $\boldsymbol{u}$, and $P_{1\mathrm{U}} f(\boldsymbol{u}, \boldsymbol{u}_1)$ and $P_{2\mathrm{U}} f(\boldsymbol{u}, \boldsymbol{u}_2)$ are the joint probability densities of fusion image $\boldsymbol{u}$ and source images $\boldsymbol{u}_1$ and $\boldsymbol{u}_2$, respectively.

Average gradient (AVG) reflects the ability to express the change of small details of the image, and

it also reflects the clarity of the fusion image. Therefore, the larger the AVG, the better the fusion image. AVG is formulated as

$$\mathrm{AVG} = \frac{1}{MN}\sum_{i=1}^{M}\sum_{j=1}^{N}\sqrt{\frac{\Delta u_x^2 + \Delta u_y^2}{2}},$$

$$\Delta u_x = u(i,j) - u(i-1,j),$$

$$\Delta u_y = u(i,j) - u(i,j-1).$$

5.2 Experiments and analysis

Experiments were carried out on four groups of source images which have been registered (Fig. 4). These source images are all classical multi-focus images and have been widely used in experiments. Fig. 5 gives the results under different fusion methods. Columns 1–6 correspond to simple averaging (AVG), discrete wavelet transform (DWT) (Pu T and Ni, 2000), CSF (Li et al., 2001), FMS (Azarang and Ghassemian, 2018), the integer-order method, and our method, respectively. In the experiments, the best fractional order for our method was chosen for comparison with other methods. The EN, MI, and AVG of images in Fig. 5 are shown in Table 2.

Figs. 5a–5f are the results of fusing the original images (Figs. 4a and 4b). After experiments, we determined that the optimal fractional order is 1.8. We use the optimal fractional order for comparison with other methods. It is observed that images obtained by the proposed integer- and fractional-order methods are clearer than those obtained by other existing methods. Based on the comparison of the three indices in Table 2, the information in fusion image Fig. 5f is the most comprehensive.

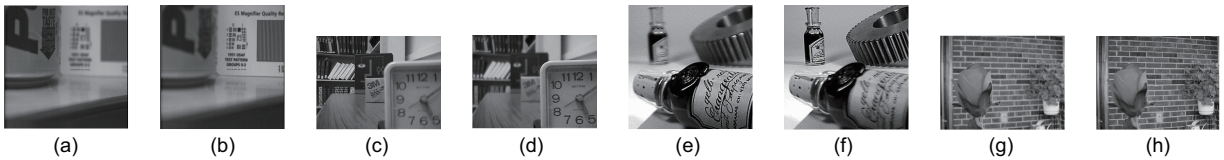

Fig. 4 Original multi-focus images: (a, b) group 1; (c, d) group 2; (e, f) group 3; (g, h) group 4

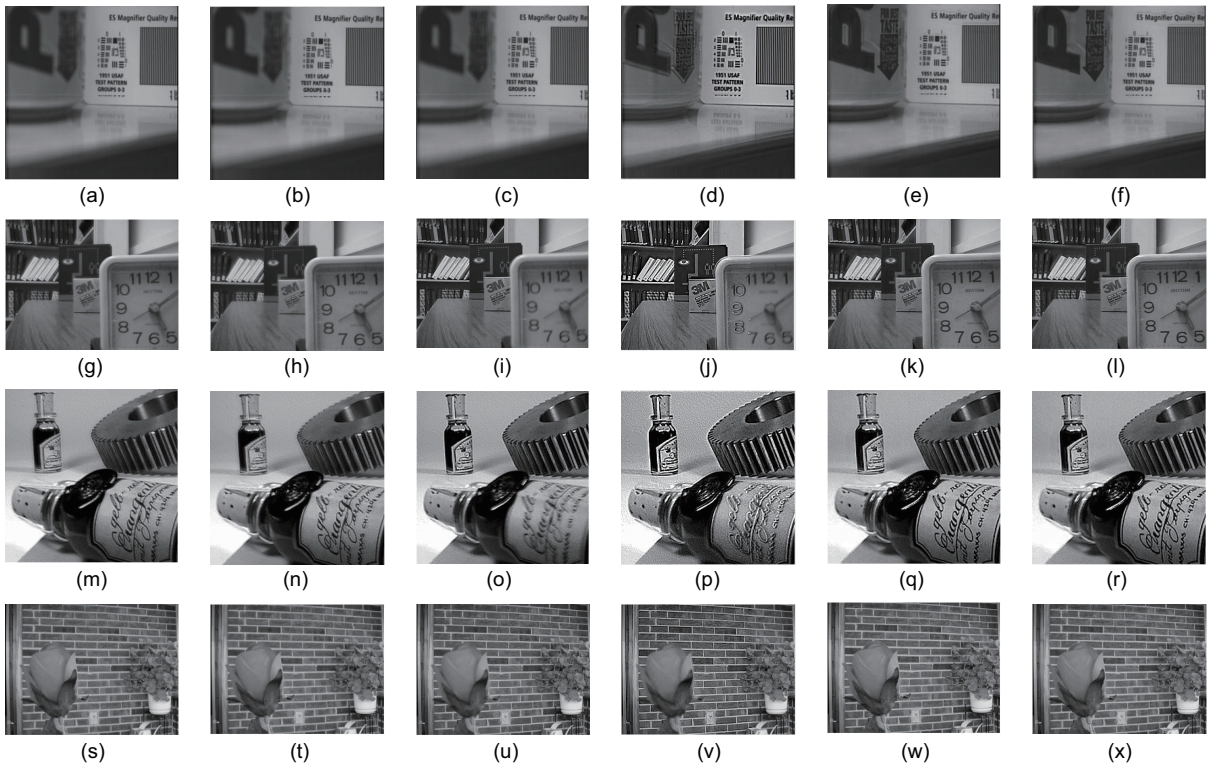

Fig. 5 Results under AVG (a, g, m, s), DWT (b, h, n, t), CSF (c, i, o, u), FMS (d, j, p, v), the integer-order method (e, k, q, w), and the proposed fractional-order method (f, l, r, x) for multi-focus images

Table 2 Performance evaluation of the fusion images in Fig. 5

Method	EN				MI				AVG			
	Group 1	Group 2	Group 3	Group 4	Group 1	Group 2	Group 3	Group 4	Group 1	Group 2	Group 3	Group 4
AVG	7.0031	7.1799	7.5265	7.1085	5.1642	4.3993	4.2203	4.0676	3.0561	4.6299	8.5841	8.6143
DWT	7.0045	7.1850	7.5335	7.1130	5.1645	4.3996	4.2122	4.0677	3.0561	4.6299	8.5841	8.6143
CSF	7.0214	7.2527	7.3806	7.1547	6.8078	6.6361	6.6302	6.3605	3.8061	5.9718	9.9415	9.9456
FMS	7.3934	7.3798	7.3335	7.4383	2.4922	2.5695	6.7939	3.1119	5.2840	5.1368	3.4203	5.7518
Integer*	7.0325	7.3244	7.5442	7.1760	5.3219	4.6989	4.6779	4.2132	4.2928	6.8383	13.2018	10.2561
Fractional*	7.0331	7.3256	7.5483	7.1766	5.3227	4.6994	4.6787	4.2096	4.2953	6.8415	13.2051	10.2570

* Methods proposed in this study. Groups 1–4 correspond to rows 1–4 in Fig. 5, respectively

Figs. 5g–5l are the results of fusing the original images (Figs. 4c and 4d). The optimal fractional order for our method is 1.4. Because of the uncertainty of digital images, artifacts will appear in image fusion. Artifact is a common problem in image fusion, closely related to the selection of fusion rules. It is observed that the method proposed in this study can avoid artifacts while the images are fused completely.

Figs. 5m–5x are the fusion results of Figs. 4e–4h. In these two experiments, the optimal fractional orders for our method are 1.1 and 1.5, respectively. Based on the perspective of human vision and the three fusion indicators, it is shown that the images fused by the proposed method contain richer information. For objects with different focusing targets, our method can clearly fuse them in a single image. We use the knowledge of the fractional-order derivative and IFS to fuse multi-focus images, and this can avoid the uncertainty of source images and preserve the details perfectly.

To highlight the advantages of FSF in image fusion, a group of special experiments were established. The FSF images of the detail layers are given in Figs. 6 and 7, and the orders of FSF are 1.0, 1.2, 1.5, 1.7, and 1.9. The EN, MI, and AVG of images fused by the proposed fractional-order method with different orders are shown in Figs. 8, 9, and 10, respectively.

When the order of FSF is 1.0, FSF is equal to the classical SF. Figs. 6 and 7 show that with the increase of fractional order, the effect of the detail layers described by FSF has improved. The use of the fractional-order derivative makes the textures of the image more obvious, and the details of the image more abundant. Therefore, FSF is more conducive to multi-focus image fusion.

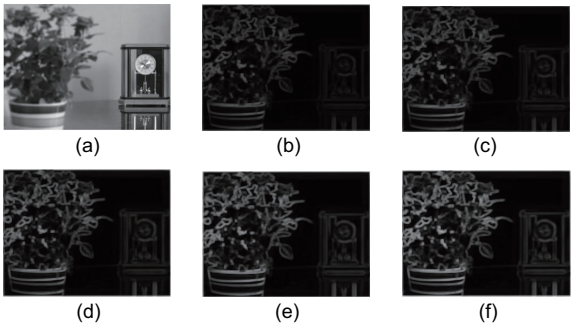

Fig. 6 FSF images of detail layer 1: (a) original image; (b) $\alpha = 1.0$; (c) $\alpha = 1.2$; (d) $\alpha = 1.5$; (e) $\alpha = 1.7$; (f) $\alpha = 1.9$

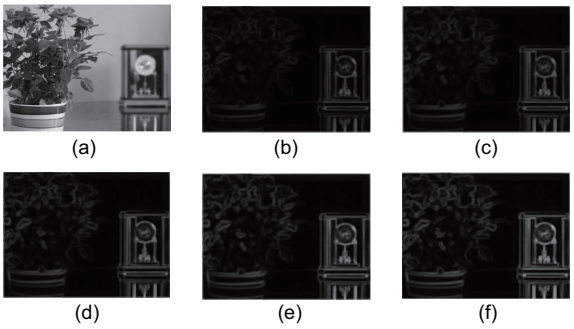

Fig. 7 FSF images of detail layer 2: (a) original image; (b) $\alpha = 1.0$; (c) $\alpha = 1.2$; (d) $\alpha = 1.5$; (e) $\alpha = 1.7$; (f) $\alpha = 1.9$

Figs. 8–10 are the performance comparison of FSF with different orders. We can conclude that the order of the best performance is about 1.5, and the corresponding fusion image is clearer than the integer one. The advantages of FSF are well reflected in this group of comparative experiments. Because FSF uses the fractional-order derivative, it is more sensitive to information and has better memory for image information than SF.

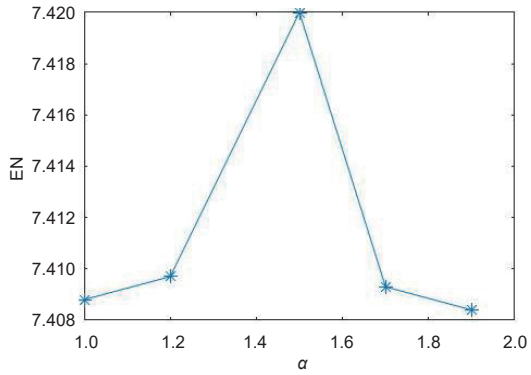

Fig. 8 The EN of the proposed fractional-order method with various orders

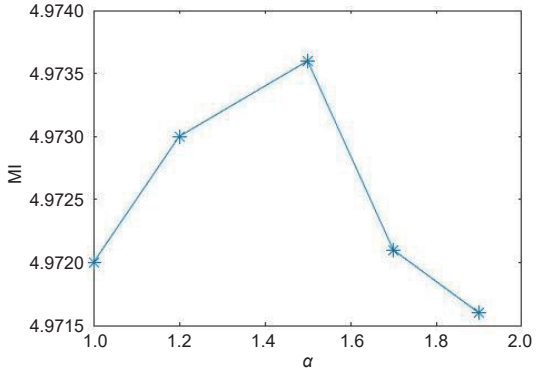

Fig. 9 The MI of the proposed fractional-order method with various orders

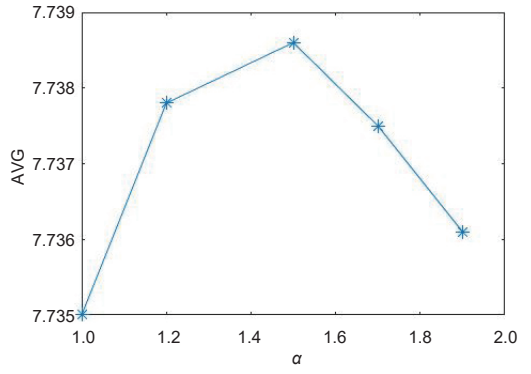

Fig. 10 The AVG of the proposed fractional-order method with various orders

6 Conclusions

In this paper, we have proposed a novel model for multi-focus image fusion. This new approach is based on two-scale image decomposition, by which an image is decomposed into two layers by average filtering. Then, the base layers are fused in IFS. This can solve the uncertainty problem effectively. The detail layers are fused in FSF. FSF is a measurement of clarity. It combines SF and a fractional-order derivative to indicate the clarity of the image. Finally, the fused multi-focus image is obtained by image reconstruction. The experimental results demonstrated that the proposed method is more effective than and superior to other classical fusion methods for multi-focus image fusion.

Contributors

Xue-feng ZHANG and Hui YAN designed the research. Hui YAN processed the data. Hui YAN and Hao HE drafted the manuscript. Xue-feng ZHANG and Hui YAN revised and finalized the paper.

Compliance with ethics guidelines

Xue-feng ZHANG, Hui YAN, and Hao HE declare that they have no conflict of interest.

References

Atanassov KT, 1986. Intuitionistic fuzzy sets. *Fuzzy Sets Syst*, 20(1):87-96. https://doi.org/10.1016/S0165-0114(86)80034-3

Azarang A, Ghassemian H, 2018. Application of fractional-order differentiation in multispectral image fusion. *Remote Sens Lett*, 9(1):91-100. https://doi.org/10.1080/2150704X.2017.1395963

Bai J, Feng XC, 2007. Fractional-order anisotropic diffusion for image denoising. *IEEE Trans Image Process*, 16(10):2492-2502. https://doi.org/10.1109/TIP.2007.904971

Balasubramaniam P, Ananthi VP, 2014. Image fusion using intuitionistic fuzzy sets. *Inform Fus*, 20:21-30. https://doi.org/10.1016/j.inffus.2013.10.011

Baleanu D, Wu GC, 2019. Some further results of the Laplace transform for variable-order fractional difference equations. *Fract Calc Appl Anal*, 22(6):180-192. https://doi.org/10.1515/fca-2019-0084

Chen DL, Chen YQ, Xue DY, 2015. Fractional-order total variation image denoising based on proximity algorithm. *Appl Math Comput*, 257:537-545. https://doi.org/10.1016/j.amc.2015.01.012

Chen Y, Qin Z, 2015. Gradient-based compressive image fusion. *Front Inform Technol Electron Eng*, 16(3):227-237. https://doi.org/10.1631/FITEE.1400217

Eskicioglu AM, Fisher PS, 1995. Image quality measures and their performance. *IEEE Trans Commun*, 43(12):2959-2965. https://doi.org/10.1109/26.477498

Huang W, Jing ZL, 2007. Multi-focus image fusion using pulse coupled neural network. *Patt Recogn Lett*, 28(9):1123-1132. https://doi.org/10.1016/j.patrec.2007.01.013

Li ST, Yang B, 2008. Multifocus image fusion using region segmentation and spatial frequency. *Image Vis Comput*, 26(7):971-979. https://doi.org/10.1016/j.imavis.2007.10.012

Li ST, Kwok JT, Wang YN, 2001. Combination of images with diverse focuses using the spatial frequency. *Inform*

Fus, 2(3):169-176.
https://doi.org/10.1016/s1566-2535(01)00038-0

Li ST, Kang XD, Hu JW, 2013. Image fusion with guided filtering. *IEEE Trans Image Process*, 22(7):2864-2875.
https://doi.org/10.1109/TIP.2013.2244222

Podlubny I, 1999. Fractional Differential Equations: Mathematics in Science and Engineering. Academic Press, San Diego, USA.

Pu T, Ni GQ, 2000. Contrast-based image fusion using the discrete wavelet transform. *Opt Eng*, 39(8):2075-2082.
https://doi.org/10.1117/1.1303728

Pu YF, Wang WX, 2007. Fractional differential masks of digital image and their numerical implementation algorithms. *Acta Autom Sin*, 33(11):1128-1135 (in Chinese).

Pu YF, Zhou JL, Yuan X, et al., 2010. Fractional differential mask: a fractional differential-based approach for multiscale texture enhancement. *IEEE Trans Image Process*, 19(2):491-511.
https://doi.org/10.1109/TIP.2009.2035980

Tao R, Deng B, Wang Y, 2006. Research progress of the fractional Fourier transform in signal processing. *Sci China Ser F*, 49(1):1-25.
https://doi.org/10.1007/s11432-005-0240-y

Wu GC, Deng ZG, Baleanu D, et al., 2019. New variable-order fractional chaotic systems for fast image encryption. *Chaos*, 29(8):083103.
https://doi.org/10.1063/1.5096645

Xu ZS, 2007. Intuitionistic fuzzy aggregation operators. *IEEE Trans Fuzzy Syst*, 15(6):1179-1187.
https://doi.org/10.1109/TFUZZ.2006.890678

Yang B, Li ST, 2007. Multi-focus image fusion based on spatial frequency and morphological operators. *Chin Opt Lett*, 5(8):452-453.

Yang Y, Que Y, Huang SY, et al., 2016. Multimodal sensor medical image fusion based on type-2 fuzzy logic in NSCT domain. *IEEE Sens J*, 16(10):3735-3745.
https://doi.org/10.1109/JSEN.2016.2533864

Zadeh LA, 1965. Fuzzy sets. *Inform Contr*, 8(3):338-353.
https://doi.org/10.1016/S0019-9958(65)90241-X

Zhang L, Liu P, Liu YL, et al., 2010. High quality multi-focus polychromatic composite image fusion algorithm based on filtering in frequency domain and synthesis in space domain. *J Zhejiang Univ-Sci C (Comput & Electron)*, 11(5):365-374. https://doi.org/10.1631/jzus.C0910344

Zhang XF, Chen YQ, 2018. Admissibility and robust stabilization of continuous linear singular fractional order systems with the fractional order α: the $0<\alpha<1$ case. *ISA Trans*, 82:42-50.

Zhu K, Liu G, Zhao L, et al., 2017. Label fusion for segmentation via patch based on local weighted voting. *Front Inform Technol Electron Eng*, 18(5):680-688.
https://doi.org/10.1631/FITEE.1500457